Automatika

Journal for Control, Measurement, Electronics, Computing and Communications

ISSN: 0005-1144 (Print) 1848-3380 (Online) Journal homepage: http://www.tandfonline.com/loi/taut20

Identification model and PI and PID controller design for a novel electric air heater

S. Álvarez de Miguel, J. G. Mollocana Lara, C. E. García Cena, M. Romero, J. M. García de María & J. González-Aguilar

To cite this article: S. Álvarez de Miguel, J. G. Mollocana Lara, C. E. García Cena, M. Romero, J. M. García de María & J. González-Aguilar (2017) Identification model and PI and PID controller design for a novel electric air heater, Automatika, 58:1, 55-68, DOI: 10.1080/00051144.2017.1342958

To link to this article: https://doi.org/10.1080/00051144.2017.1342958

Published online: 07 Jul 2017.

AUTOMATIKA, 2017
VOL. 58, NO. 1, 55–68
https://doi.org/10.1080/00051144.2017.1342958

Taylor & Francis
Taylor & Francis Group

REGULAR PAPER

OPEN ACCESS Check for updates

Identification model and PI and PID controller design for a novel electric air heater

S. Álvarez de Miguel [a,b], J. G. Mollocana Lara[a,c], C. E. García Cena[b,c], M. Romero[a], J. M. García de María[b] and J. González-Aguilar[a]

[a]High Temperature Processes Unit, IMDEA Energy Institute, Móstoles, Madrid, Spain; [b]Escuela Técnica Superior de Ingeniería y Diseño Industrial, Universidad Politécnica de Madrid, Spain; [c]Centre for Automation and Robotics, CSIC-UPM, Spain

ABSTRACT

In this article, the software and hardware control architecture for a novel high-temperature three-phase electric air heating furnace is presented. It consists of a multiple-input single-output (MISO) nonlinear plant designed to heat air at flow rates in a range between 10 and 60 Nm^3/h, from ambient temperature up to 1000 °C.

A divide-and-conquer (D&C) approach is applied. It consists in discretizing the air flow rates and working temperatures in intervals where the system behaviour is considered as single-input single-output (SISO) linear plant. Process identification techniques have been used to obtain empiric models for different operation ranges of the electric furnace. The controller parameters have been calculated using the Ziegler–Nichols tuning method.

The resulting output air temperature control is composed of a set of 12 PI and PID controllers. The switch among controllers as a function of air flow rates and temperatures is carried out using programming logic and gain scheduling technique, respectively. The resulting multiple controller has been tested under real conditions and the results are presented and discussed.

ARTICLE HISTORY
Received 21 February 2017
Accepted 9 June 2017

KEYWORDS
High-temperature air heater; PI controllers; PID controllers; thermochemical heat storage test rig; three-phase electric air heating furnace

1. Introduction

Temperature control is a challenging issue in technological processes in many branches of industry. For example, temperature control in air heating systems is widely used in metallurgic, chemical or pharmaceutical industries. One of the most popular control algorithms, the proportional-integral-derivative (PID) structure, has been successfully applied in many processes for temperature control purposes because of its simplicity and robustness.

Classic PID schemes and controllers have been updated and enhanced over the years, from the early controllers, based on relays and synchronous electric motors or pneumatic or hydraulic systems to current microprocessors. The latest improvements in the field of PID tuning are the development of the setpoint overshoot method in the closed-loop approach [1] and the direct synthesis method in the open-loop approach. The latest method has been evaluated in various unstable processes with time delay obtaining nominal and robust control performances, improving closed-loop approach performances, and reducing the undesirable overshoot [2]. There have also been software developments, such as the inclusion of gain scheduling of PID controllers, which dynamically adjust the gains of the PID algorithm during the control process [3], or real-time implementations in languages like Matlab [4] or LabVIEW [5].

Even so, electric furnaces' large inertia, time delay, nonlinear and time-varying characteristics have been the motor for the development of more advanced control schemes. In [6], a temperature controller is developed based on the combination of fuzzy and PID control. In [7], a fuzzy controller is designed through the application of an adaptive genetic algorithm for PID parameter's optimization. In [8], the fuzzy adaptive control is combined with a grey prediction control to develop a grey prediction fuzzy adaptive control. In these three studies, advanced controllers for furnaces without air flow heating are simulated as well as the pertinent conventional PID control for comparison purposes. Although there is no clear definition of the temperature application range, simulated results show no quantified better performances of the advanced control schemes compared to the conventional PID controllers.

A fuzzy logic controller is optimized for an electric air heater system in [9]. There is no indication of the air flow rate used in the simulation but the controller performance was evaluated with a setpoint change from 30 to 120 °C. This work shows an insight of the complexity in the optimization of the fuzzy logic control (FLC) with the evaluation of five types of

CONTACT J. González-Aguilar jose.gonzalez@imdea.org

membership function with four different sizes of rule base. There is no comparison with a PID controller, but the results indicate that 15 out of the 20 simulated controllers have an average overshoot of 20 °C. In addition, four of the controllers do not reach the set-point in 200-min time, and only the fuzzy logic controller with combined trapezoid and triangular membership function and 3 × 3 rule achieves an over-damped temperature response after 178-min time.

Four different control schemes are optimized and compared in an air heater plant in [10]. The air flow used is not indicated, but the study is based on the model obtained from an open-loop step response from 30 to 55 °C. This model is used to design a PID control strategy. The knowledge of the optimal PID controller design is used to develop an FLC scheme. The membership values are optimized using genetic algorithms (GA) in conjunction with FLC. Scale mapping is performed using triangular membership function with the help of artificial neural networks (ANNs). The ANN models developed for fuzzification of input variables are used in neuro-fuzzy control (NFC) scheme. The comparison of the above controller's closed-loop responses shows in terms of integral error criteria that NFC has the best performance closely followed by FLC-GA, PID and FLC. In terms of integral time absolute error, the controller order from the fastest to the slowest is NFC, FLC-GA, FLC and PID.

Nevertheless, many modern controllers on the market are based on a PID structure. According to a survey conducted in 2010, the ratio between PID, conventional advanced and model predictive controls is about 100:10:1 [11].

In order to get the control law, the first step is to define the desired output response $y(s)$ of a particular system to an arbitrary input $u(s)$ over a time interval, which is done by system identification [12]. Sometimes, it is possible to obtain a model based on a complete physical description of the system; however, this model is complex and the computational cost to solve it is high [13]. The second step is to determine the PID controller parameters; there is extensive literature about methods for tuning of PID controllers for different controller structures and from different approaches; a vast collection can be found in [14].

This paper deals with the identification model and control architecture for a novel air heating system. This system was specially designed and developed to recreate the specific experimental conditions of a high-temperature air solar power plant [15]. Thermochemical energy storage materials and the performance of their reactions are tested there, so the temperature control is crucial for the successful material evaluation.

Taking into account the state-of-the-art presented above, the main contributions of this paper are as follows:

- Experimentally identify the model of a novel electric air heating system. Due to the nonlinearity of the model, an input–output methodology is applied, and the model is linearized in different operational points.
- Design and validate by experimental testing in the real plant, PI and PID controllers for each one of the ranges defined with a gain scheduling procedure implemented to have a smooth switch between controllers.
- Analyze the control behaviour of the plant in a wide range of well-defined temperatures and air-flow rates.
- Evaluate control performance, not only regarding the controllers' optimized parameter values, but also considering the intrinsic behaviour of the furnace and the differences between the working conditions and the optimal design conditions.

This paper is organized as follows: Section 2 describes the process to be controlled and includes the main characteristics of its hardware and software. Section 3 presents the complexity of the plant and the control design methodology applied, which is done by model identification and controller design. Section 4 focuses on the experimental results obtained; a graphical user interface (GUI) and several control evaluation tests. And, Section 5 encompasses the main conclusions obtained from the work presented in this paper.

2. Process description

Research and development activities usually need the design and construction of test facilities to create specific and well-controlled experimental conditions. Álvarez de Miguel et al. presented a 100-Wh multipurpose particle reactor for thermochemical heat storage in concentrating solar power plants [16]. The experimental facility is located at the IMDEA Energy Institute, Móstoles, Madrid, Spain. This installation required a novel air heater capable to produce an air flow rate in the range from 10 to 60 Nm^3/h, at a defined temperature value from ambient temperature up to 1000 °C. In order to control the desired outlet temperature and air flow rates, it is necessary to develop a model.

The facility comprises a chemical particle reactor and its test bench; a picture and a design scheme are shown in Figure 1. The objective of the test bench is the production of hot air, which is used to heat up the materials introduced in the reactor [17]. The reactor can work as a fixed bed or as a fluidized bed reactor depending on the air flow going through it. The storage material is placed into the reactor and the desired experimental conditions are defined in the test bed computer.

As shown in the process flow diagram in Figure 2, the test bed is made of several industrial components such as

- Industrial compressor (Atlas Copco), which provides compressed air for the setup.

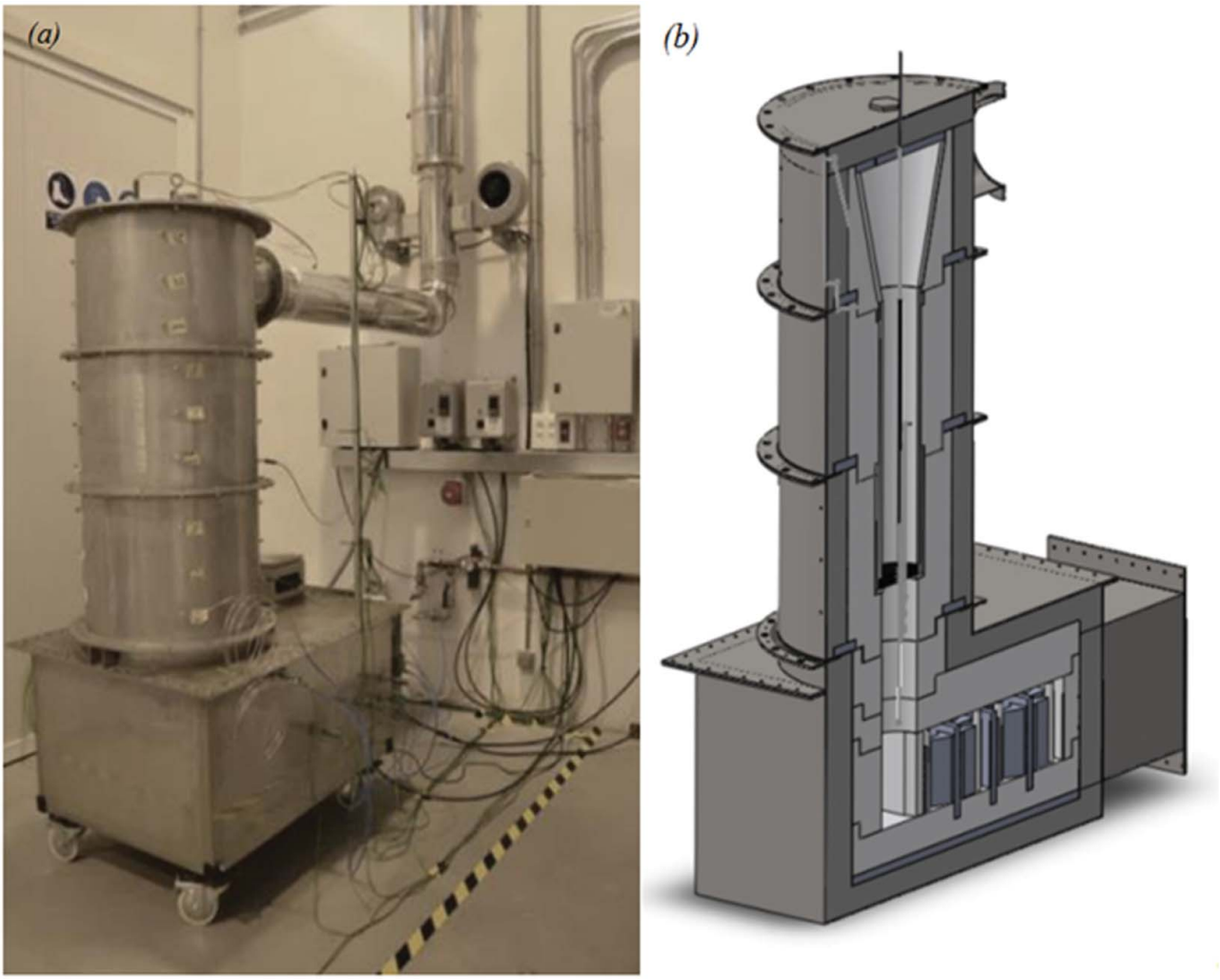

Figure 1. (a) Photograph and (b) design scheme of the 100-Wh thermochemical storage installation.

- Two commercial mass flow controllers (Bronkhorst High-Tech) used to set the working air flow rate defined in each experiment.
- Air heating system that provides hot air at the test temperature selected for every air flow rate in use. It is composed of two stages:
  - Peripheral electric resistances or preheaters that comprise two commercial devices from Osram Sylvania, controlled by commercial SureHeat JET controllers, which are used for the most demanding experiment conditions. Each preheater can heat a maximum of 30 Nm^3/h of air from ambient temperature up to 500 °C.
  - Main heater: a three-phase electric furnace designed ad hoc; a 16 kW device composed of a set of three resistors arranged in star and made out of Resistohm PRM from Aperam. The power through resistors is regulated by a commercial three-phase power regulator from SRC.
- The resistors are located in the core of an insulating material structure with an inside-tunnel configuration; the gas stream flows through it while its temperature is increased, maintained or decreased according to the experiment requirements.
- Gas analysis equipment from Siemens, connected downstream of the reactor: the materials to be tested would react with the oxygen of the air, so that the gas analyzer is used to quantify the oxygen content in the process gas once it has passed through the reactor.

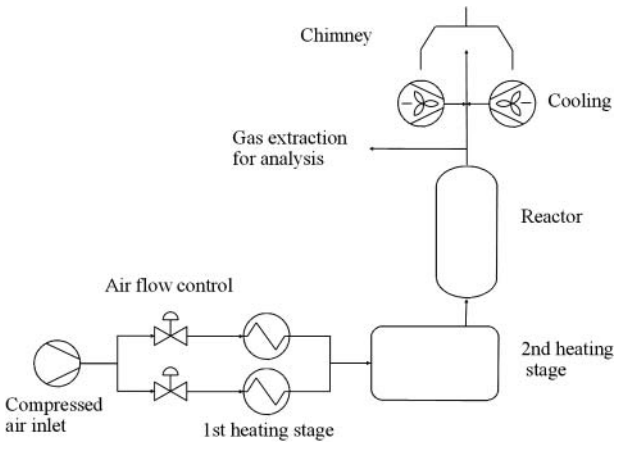

Figure 2. Process flow diagram.

- Cooling system to adjust the temperature of the exhaust gas prior to its release. The cooling is done by mixing the exhaust gasses with room temperature gas flow produced by the application of two air blowers from EBM.

The reactor is equipped with a total of 19 K-type thermocouples located at different heights and radial depths of the reactor body. The electric furnace has a total of seven K-type thermocouples; five of them are placed at different locations along the gas path; one is used to activate an alarm in case of high-temperature damage risk, and the remaining thermocouple is used for control purposes.

Reactor and furnace are equipped with differential pressure gauges that monitor the pressure variations caused by air flow rate and temperature changes while the one in the reactor is also used to study the fluidization properties of the material under evaluation. The test facility also includes a relative pressure meter, installed underneath the sieve at the bottom of the reactor.

The experimental implementation of the control hardware, the interrelations among the air flow and temperature controllers of the above-described equipment and the measurement points in the system are detailed in the piping and instrumentation diagram (P&ID) shown in Figure 3.

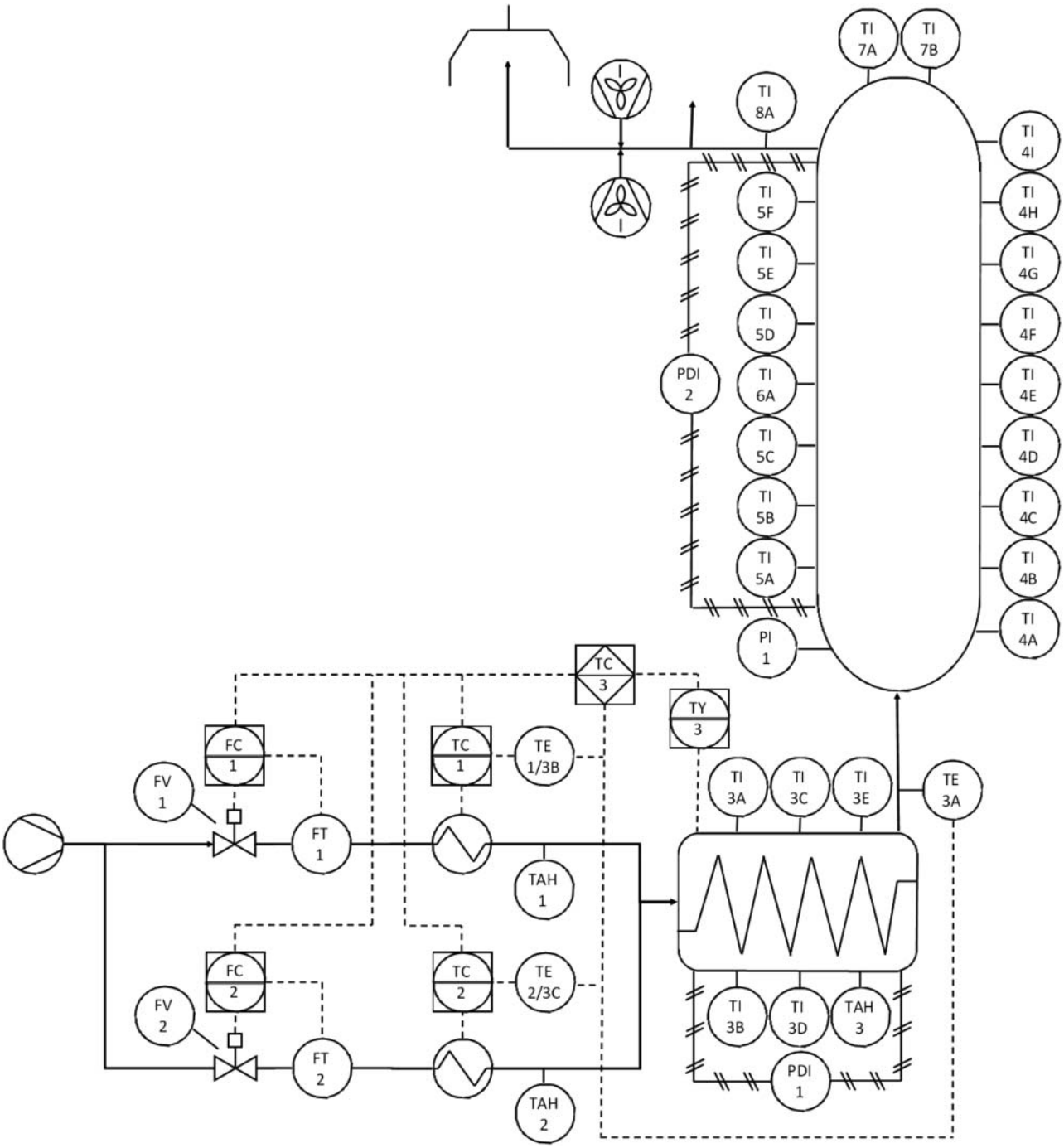

Figure 3. P&ID of the test rig.

The control system also includes a CompactRIO 9074 (cRIO) from National Instruments, the required input/output modules and a computer communicating with the cRIO via Ethernet. The data acquisition system records all the signals for every second of the experiment, and keeps them in a text file for further analysis.

The control and data acquisition system also manages other variables, such as setpoint and output values for the flowmeter, temperatures related to the preheaters, gas compositions from the analyzer and control of the three-phase electric furnace.

3. Model and control of the air heater

Heating processes involving electric resistance furnaces are usually slow and may combine several nonlinear features. Thus, obtaining the physical model that mathematically describes the system is usually discarded, because of its high complexity, in favour of the black box approach for process identification.

Based on practical knowledge of the air heater, the plant can be identified as a multiple-input single-output (MISO) nonlinear plant: the outlet temperature depends on the air inlet temperature, the air flow rate and the power provided to the furnace resistors.

Peripheral electric resistances are only used for extreme experimental requirements. So, in order to develop the control of the three-phase electric furnace, the air inlet temperature can initially be considered as a simple perturbation on the system.

By discretizing the air flow rates in three different ranges, the effects of nonlinear distortion get small enough to be considered as a disturbance for the system, so the plant becomes a single-input single-output (SISO) nonlinear system, where the air outlet temperature depends only on the furnace electric power. The switch among air flow ranges is carried out using a decision programing structure.

These dependency relations are presented in the block diagram of the process shown in Figure 4. The elements included into the dotted-line rectangle correspond to the furnace controller, the CompactRIO, named TC/3 in Figure 3. The rest of the features in the block diagram are explained below:

- $r(s)$ is the desired air outlet temperature value, the setpoint.
- $y(s)$ is the process variable, the real temperature value at the outlet of the furnace.
- $h(s)$ is a voltage signal equivalent to $y(s)$. It is generated by the thermocouple, named TE/3A in Figure 3, and used by the gain scheduling to determine the control parameters – K_p, T_i and T_d – as function of the defined operating process point.
- $e(s)$ is the error signal, which is the difference between the desired and real values of the temperature. It is calculated as $r(s) - h(s)$.
- Q represents the perturbation of plant caused by the air inlet flow rate. Its value results from the addition of the air delivered by the air flow controllers, named as FC/1and FC/2 in Figure 3.
- T_o represents perturbation of the plant caused by the temperature of the air measured at the inlet of the furnace. It is the average value between the temperatures acquired from sensors TE 1/3B and TE 1/3C in Figure 3.
- $u(s)$ is the controller output signal. It is the voltage signal that reaches the actuator of the system, identified as TY/3 in Figure 3.
- $c(s)$ is the current signal generated by the actuator, which is responsible for the variation over the electric power supplied to the furnace resistors.

Nevertheless, the process is still quite complex, because of its nonlinear character and dependency on the process outlet temperature. To tackle this problem, the working temperature range is divided into several sections where the plant behaviour is assumed to be linear.

A gain schedule (GS) structure is implemented in order to choose the appropriated PID controller to soften the switch between the working temperature sections in each of the air flow ranges. Depending on the reaction temperatures of the thermochemical material to be tested in the reactor, the full temperature

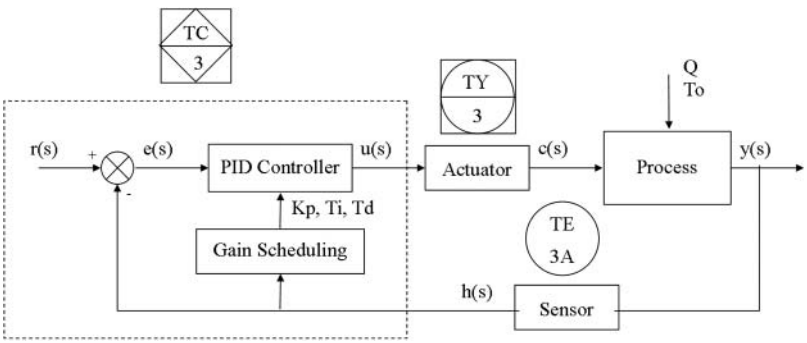

Figure 4. Process block diagram.

scale is divided into ranges of 200 °C. The exact values of the working temperature sections are defined during the identification process of the plant.

Therefore, the methodology applied to define the process control is to regulate the MISO nonlinear plant using several SISO linear controllers. This is done in two steps: first, system identification of the plant is done for each of the air flow ranges and their corresponding temperature sections; and, second, control parameter values are determined by tuning the controllers.

3.1. Model identification of the air heater

As it was explained in Section 1, the model of this kind of processes is nonlinear, and hence input–output methodology was used and a model for each operation point was identified. Experiments conducted for data collection consisted of open-loop responses to step variation of the furnace power. Considering the experimental requirements for the reactor tests to be performed on the thermochemical storage materials, and also taking into account the lower air heat transfer coefficient observed at small air flow rates, three air flow rate intervals are defined: 10–20, 20–40, and 40–60 Nm^3/h. The flow rates used in each experiment were set to the middle point of the ranges 15, 30, and 50 Nm^3/h, respectively. Each step variation is generated consecutively and starts once the previous step response has reached the steady state. The temperature sections for each air flow range are determined by the temperature at which steady state is reached.

Figure 5 shows the working scheme developed for the identification process. Figure 6 shows an example of the step-response experiment. In the intermediate air flow range, the temperature sections resulted to be from ambient temperature to 240 °C, from 240–420 °C, 420–745 °C, and 745–1000 °C.

Matlab System Identification Tool was used to evaluate several empirical process models for each step response. The time delay of the system, T_d, was graphically determined for each step response and introduced as a known parameter in the system identification tool. Then, the system responses were fitted into first-order plus time-delay (FOPTD) (1); second-order plus time-delay (SOPTD) (2), and third-order plus time-delay (TOPTD) (3). By running the Matlab System Identification Tool for each step response with one, two and three poles, the static gain K_c, and the value of the poles T_{p1}, T_{p2}, and T_{p3}, respectively, were obtained.

$$G(s) = \frac{K_c}{T_{p1}s + 1} e^{-T_d s} \quad (1)$$

$$G(s) = \frac{K_c}{(T_{p1}s + 1)(T_{p2}s + 1)} e^{-T_d s} \quad (2)$$

$$G(s) = \frac{K_c}{(T_{p1}s + 1)(T_{p2}s + 1)(T_{p3}s + 1)} e^{-T_d s} \quad (3)$$

The selection among the three models obtained for each step is based on the similarity principle: a curve of data is produced with each of the models, and the model that produces the closest curve to the experimental data is selected. As an example of this model

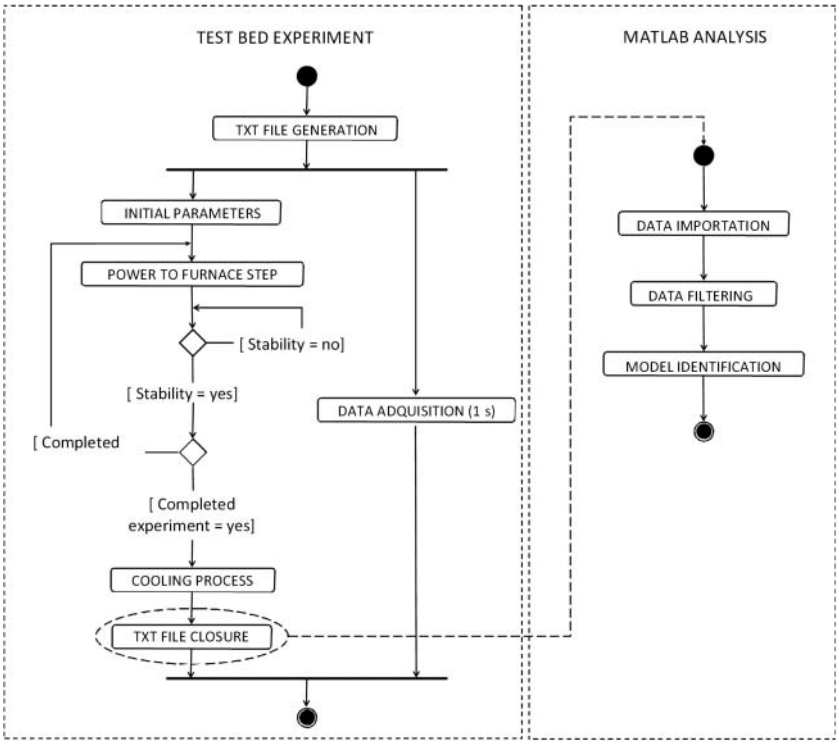

Figure 5. Identification process scheme.

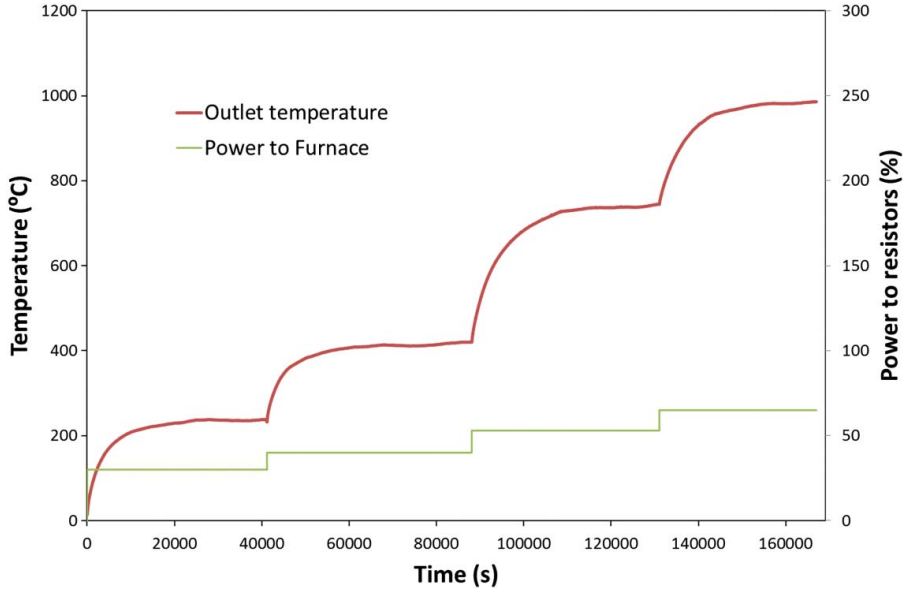

Figure 6. Step response for 20–40 Nm^3/h flow range.

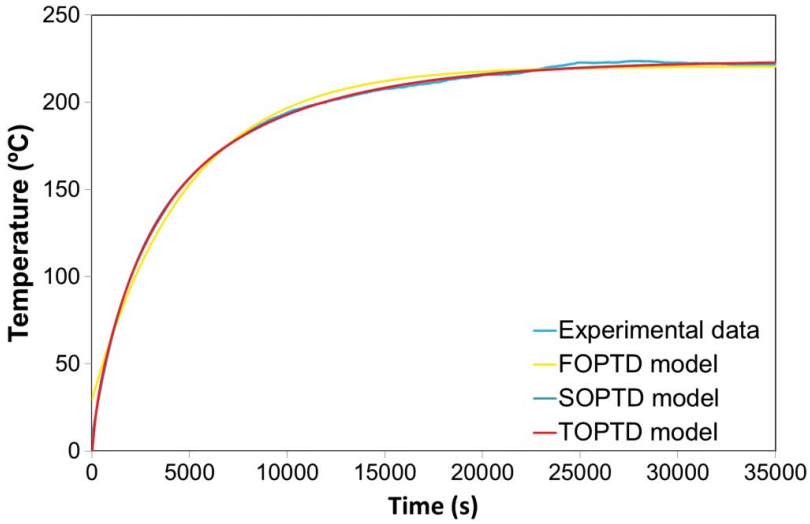

Figure 7. Model validation for the second temperature step in the 20–40 Nm^3/h air flow range.

validation process, Figure 7 shows the obtained models comparison for the first temperature step measured in the 20–40 Nm^3/h air flow range. In this case, the TOPTD model has a similarity to the experimental data of 97.06%, higher than the SOPTD and the FOPTD, which have 96.76% and 90.90%, respectively. Thus, the TOPTD parameters are retained for the posterior design of the controller.

For concision purposes, only the selected models and their corresponding parameters are shown in Tables 1–3. Information related to discarded models can be found in [18].

3.2. Design of the temperature controllers

Once the model identification of the air heater is completed, the most similar to the experimental data

Table 1. Step response model parameters for the 10–20 Nm^3/h air flow range.

Model Temperature section (°C)	TOPTD Amb.T–210	SOPTD 210–475	SOPTD 475–810	SOPTD 810–1000
K_c	9.25	26.62	33.81	37.14
T_{p1}	14,720	29,722	27,816	16,042
T_{p2}	1795.9	6339.7	6081.2	1776
T_{p3}	98.00	–	–	–
T_d	8	4	24	12

Table 2. Step response model parameters for the 20–40 Nm^3/h air flow range.

Model Temperature section (°C)	TOPTD Amb.T–240	SOPTD 240–420	SOPTD 420–745	SOPTD 745–1000
K_c	7.46	18.39	24.78	22.89
T_{p1}	2171.9	8170.7	7622.6	21,951
T_{p2}	7633.3	1556.1	1150.5	3781.9
T_{p3}	198.36	–	–	–
T_d	5	6	12	14

Table 3. Step response model parameters for the 40–60 Nm^3/h air flow range.

Model Temperature section (°C)	SOPTD Amb.T–200	SOPTD 200–510	SOPTD 510–760	SOPTD 760–1000
K_c	5.64	14.73	15.28	9.89
T_{p1}	3739.1	5176.5	7820.5	10,453
T_{p2}	875.37	1042.6	1464.7	2813.8
T_d	8	2	3	8

models are chosen. Those models are used to design several P, PI and PID controllers to work in the different temperature and air flow ranges. The switch among air flow ranges is done by a programing decision structure. For a settled air flow rate, the switch among temperature ranges is done by GS. The scheduling variable is the process variable, the air temperature at the exit of the furnace.

The first step to design the controllers is to reduce the order of the models obtained in Section 3.1 to equivalent first-order models. Therefore, the process reaction curve method is implemented in Matlab R2014b, and it is used to approach the second- and third-order models curves to a FOPTD model.

The FOPTD model parameters and the resulting P, PI and PID controller parameters for each temperature section of the three flow ranges are shown in Tables 4–6.

In order to evaluate the performance of the different controllers, several simulations are done using Simulink from Matlab. The proposed control architecture implemented in Simulink environment for the comparison of the P, PI and PID controllers is shown in Figure 8.

Figure 9 shows the comparison of the controllers designed for the first temperature step in the 20–40 Nm^3/h air flow range. This operational range is used to explain the general findings in the P, PI and PID controllers' comparison. From the P controller response, a stationary state error is observed; due to the importance of reaching the desired temperature in the work bench, the P controllers are discarded. Comparing between PI and PID controllers, it is appreciated how PID controllers have smaller overshoots and shorter setting times. Nevertheless, it is commonly known that PID controllers can have a problem of derivative kick as it will be further explained in Section 4.2. Meanwhile, PI controllers have bigger overshoots and longer setting times, but as a result of their lack of the derivative term, the derivative kick risk is nullified.

The control logic is implemented in LabVIEW by means of the PID GS and PID virtual instruments. The PID GS block defines the set of parameters for the PID controller according to the process' range of operation defined by the scheduling variable, the outlet furnace's temperature. The PID virtual instrument implements the PID controller which is completed with an integrator anti-windup built in structure that uses a signal limiter to prevent the integrator from winding up, thus preventing actuator saturation, extending the furnace's useful time. The anti-wind up structure softens the transition of the control signal when a change in the PID gains is detected. The anti-wind up structure acts over the integral gain to maintain a constant exit signal with the new parameters.

4. Experimental results

4.1. User interface

To perform experimental tests, a GUI was developed. The aim of the GUI is to allow human operator to set

Table 4. FOPTD and PID parameters for the 10–20 Nm^3/h air flow range.

	FOPTD model			P	PI		PID		
Temperature section (°C)	K_c	T_{p1}	T_d	K_p	K_p	T_i	K_p	T_i	T_d
Amb.T–210	9.25	1168	19,938	1.84	1.66	3890	2.21	2336	584.2
210–475	26.62	3250	45,578	0.53	0.47	10,821	0.63	6499	1625
475–810	33.81	3130	42,861	0.40	0.36	10,422	0.49	6259	1565
810–1100	36.94	7369	53,247	0.20	0.18	24,538	0.23	14,737	3684

Table 5. FOPTD and PID parameters for the 20–40 Nm^3/h air flow range.

	FOPTD model			P	PI		PID		
Temperature section (°C)	K_c	T_{p1}	T_d	K_p	K_p	T_i	K_p	T_i	T_d
Amb.T–240	7.41	1374	15,366	1.51	1.36	4576	1.81	2748	687.1
240–420	18.39	851	12,071	0.77	0.69	2832	0.92	1701	425.3
420–745	24.78	6791	10,669	0.63	0.57	2262	0.76	1358	339.6
745–1100	22.89	2127	31,659	0.65	0.58	7083	0.78	4254	1064

Table 6. FOPTD and PID parameters for the 40–60 Nm^3/h air flow range.

	FOPTD model			P	PI		PID		
Temperature section (°C)	K_c	T_{p1}	T_d	K_p	K_p	T_i	K_p	T_i	T_d
Amb.T–200	5.64	453.85	5829	2.28	2.05	1511	2.73	907.7	226.9
200–510	14.73	558.43	7756	0.94	0.85	1860	1.13	1117	279.2
510–760	15.28	802.03	11,506	0.94	0.85	2671	1.12	1604	401.0
760–1100	9.89	1377.1	16,951	1.24	1.12	4586	1.49	2754	688.6

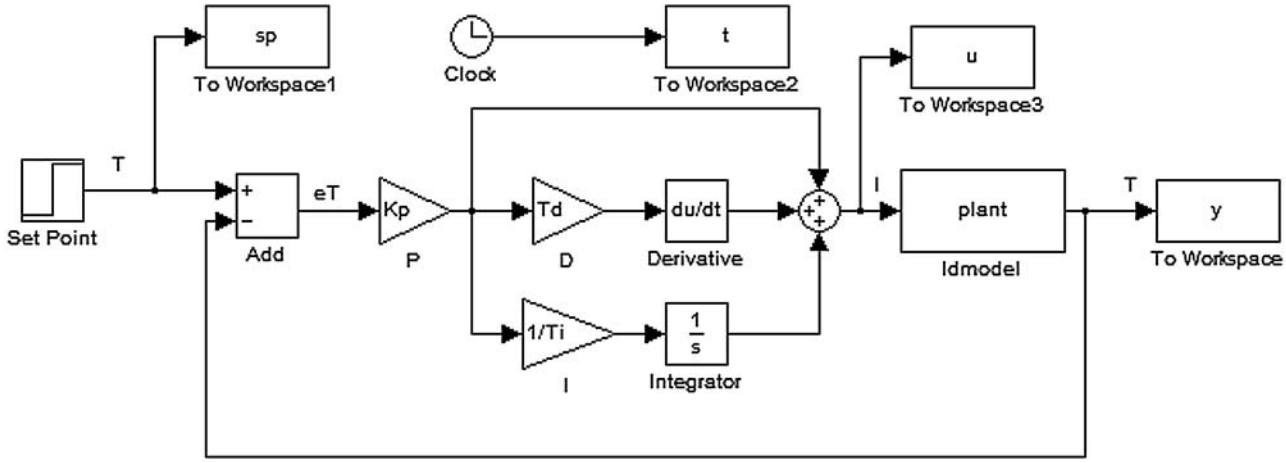

Figure 8. Block diagram implemented in Simulink to evaluate the performance of the P, PI and PID controllers.

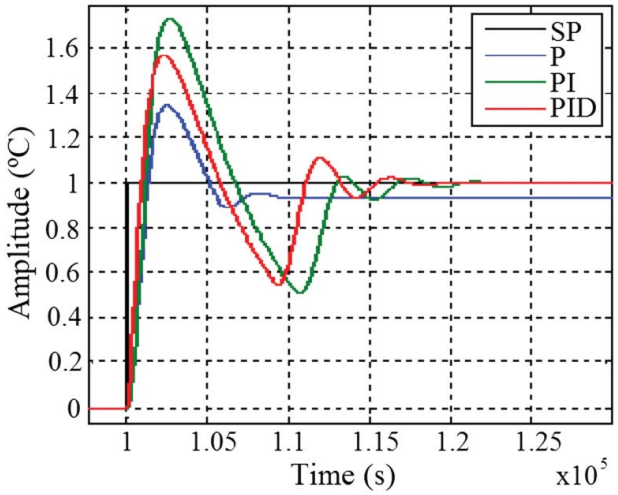

Figure 9. Simulink simulation results for the P, PI and PID controllers obtained for the first temperature step in the 20–40 Nm^3/h air flow range.

experimental conditions and to get information about the experimental tasks. This application has been developed under LabVIEW 2012 environment.

The GUI is organized into five different screens; the first one is related to the experiment management; second, third and fourth screens are displaying the information acquired from the test rig related to the air heating furnace, the preheaters and the reactor, respectively; and, the fifth screen displays the pressure and gas analysis data.

Figure 10 shows a screenshot of the experiment management slice, named process, of the GUI. Here, the human operator can start the program, by introducing a password, and define the path to the txt file where the experimental data is kept. The operator can also define the next aspects of the experiment:

- Switch on/off the furnace, preheaters and air blowers.

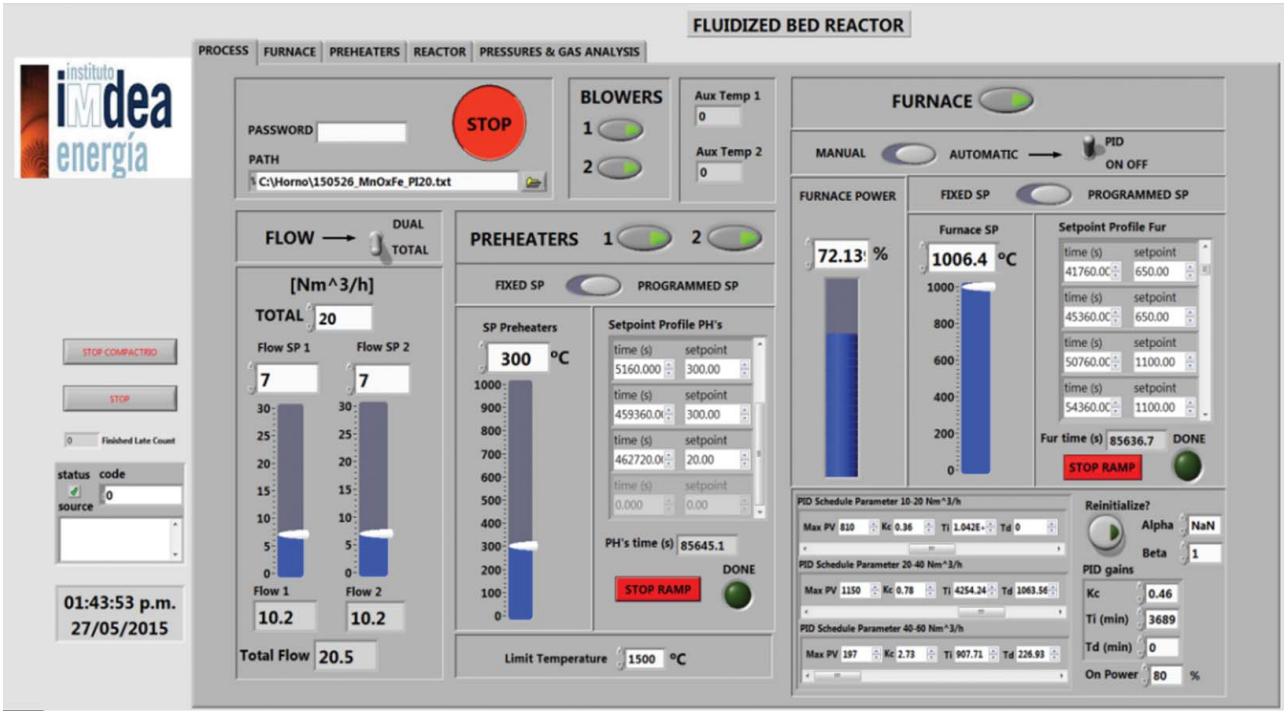

Figure 10. Screenshot from the process slice of the GUI application.

- Define the air flow setpoint. It is possible to set a total air flow or an individual setpoint for each air mass flow controller.
- Define the temperature setpoint for the preheaters as well as for the furnace. There are two options setting a fixed value or a profile. The profile would include different heating or cooling ramps and temperature plateaus.
- Selection of manual or automatic operation mode for the furnace. In the automatic operation mode, operator can choose P, PI or PID control or on/off control.
- Set the controller parameters for a P, PI or PID control in each of the three air flow ranges defined.
- Set a temperature safety value for high temperature risk. If any of the thermocouples measures a value higher than the safety one, the system is automatically switched off for the equipment integrity protection.

GUI process screen shows the total or individual air flow rates that are being fed the test rig and the value of two peripheral temperatures gathered from two K-type thermocouples fixed to the external metallic surface of the test rig.

Figure 11 shows screenshots of the four GUI data visualization slices corresponding to furnace, preheaters, reactor, and pressure and gas analysis. Each one displays graphs containing time-evolution and instant values of the recorded variables assigned to each facility section.

4.2. Performance of the designed controllers' assessment

Several experiments were conducted to evaluate the performance of the control strategy for PI and PID controllers. As material evaluation experiments require a defined temperature, P controllers are not suitable because of the steady-state error associated to them, and hence they were initially discarded.

The experiments aimed to check the developed PI and PID parameters' controls in every flow rate and temperature range. Therefore, for different constant air flow rates within each range, experiments using various temperature setpoints, such as heating/cooling rates and isotherms, were conducted. The faster heating ramp required for material evaluation experiments is 5 °C/min, and hence this value is defined for the control test experiments. In order to reach this heating rate, preheaters were set to 300 and 500 °C for the intermediate and highest air flow ranges, respectively; they were off for the lowest air flow range. Isotherms were defined at temperatures close to the maximum value for each temperature section defined in the air

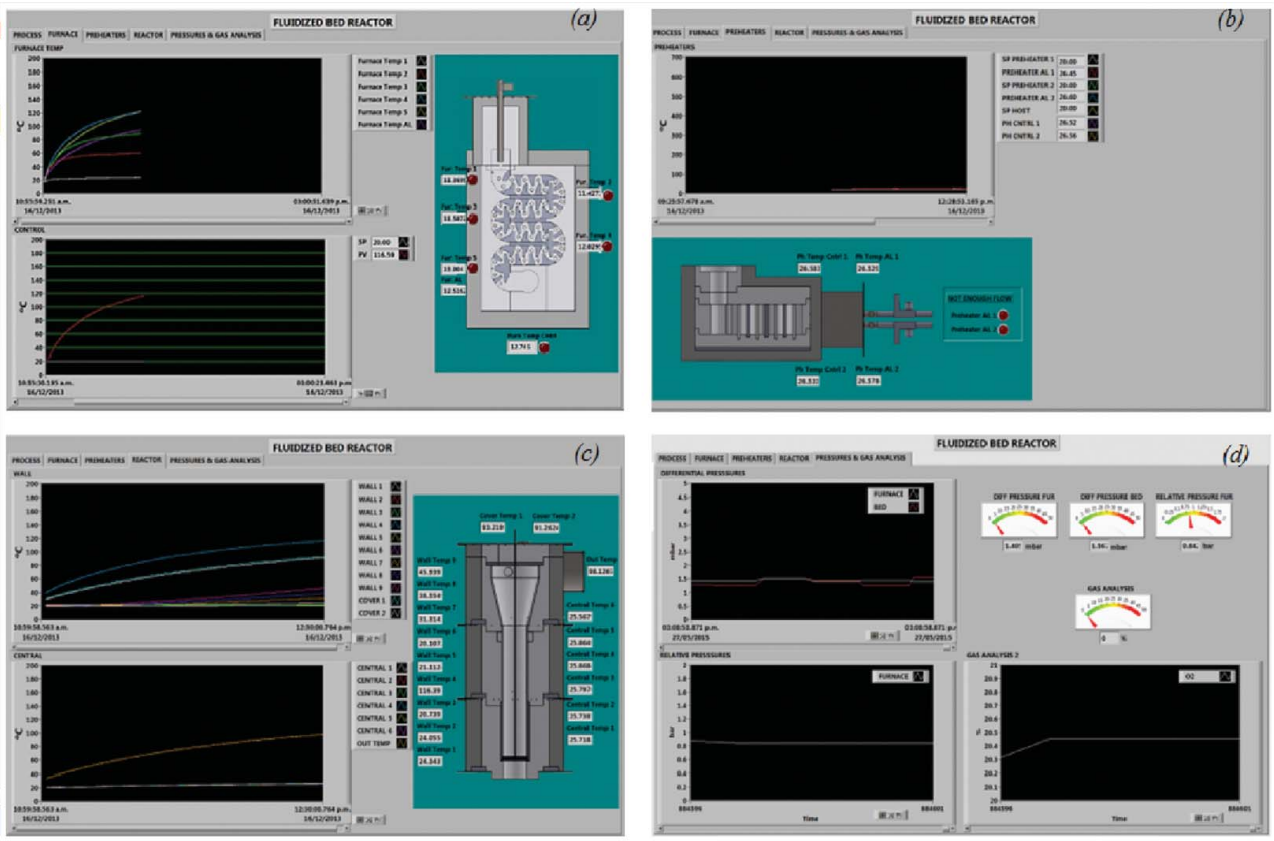

Figure 11. Screenshot from the data display slices of the GUI application: (a) furnace, (b) preheaters, (c) reactor, and (d) pressure and gas analysis data.

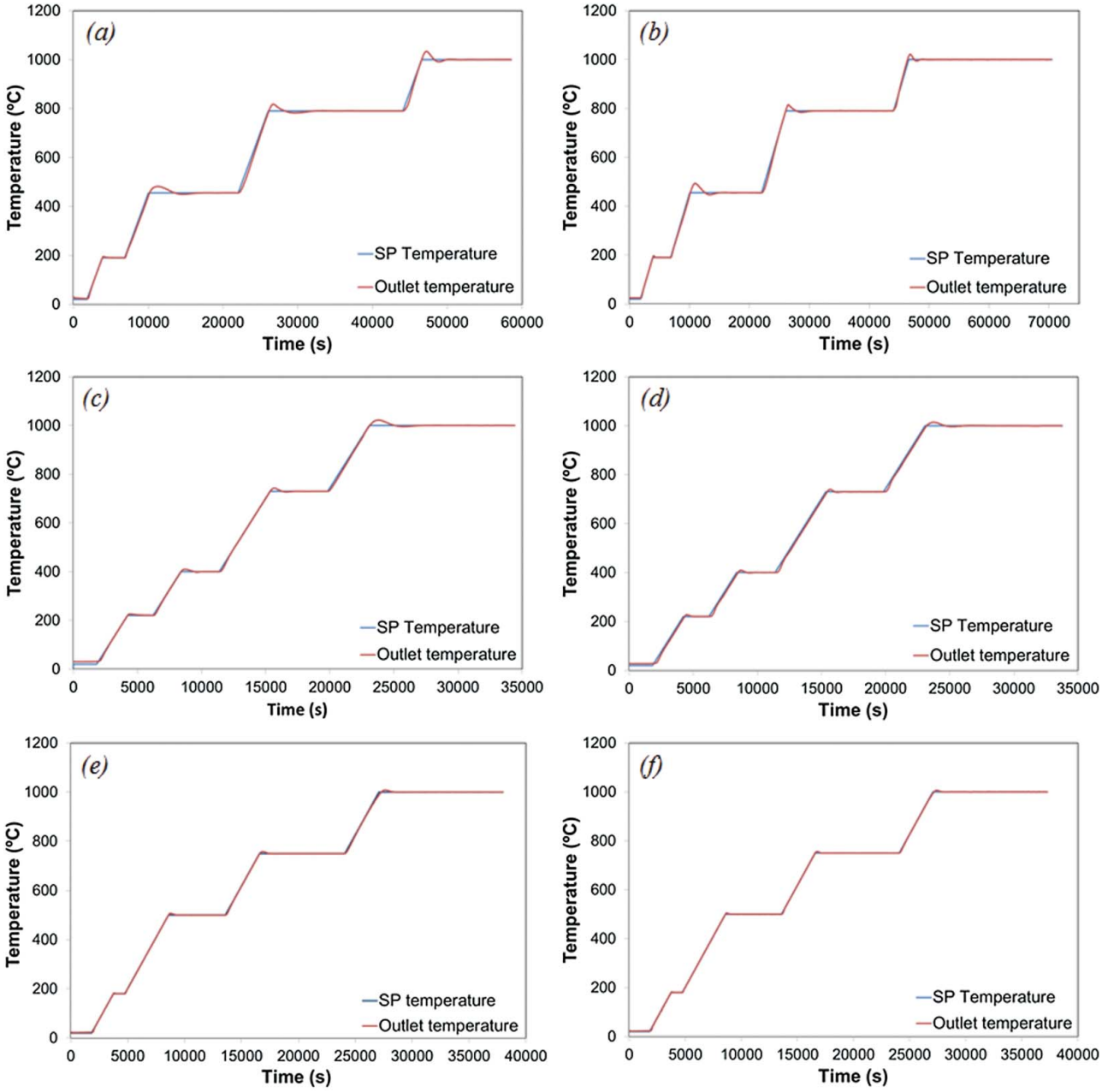

Figure 12. (a) PI and (b) PID controller evaluation in the air flow rate interval [10, 20] Nm^3/h. (c) PI and (d) PID controller evaluation in the air flow rate interval [20, 40] Nm^3/h. (e) PI and (f) PID controller evaluation in the air flow rate interval [40, 60] Nm^3/h.

flow range. Each temperature setpoint related to an isotherm was maintained fixed until the system reached steady-state conditions.

Figure 12 illustrates the PI and PID experiments conducted for each air flow range. Figure 12(a,b) shows, respectively, the PI and PID experiments at 15 Nm^3/h and temperature plateaus defined at 190, 455, 790, and 1000 °C. Figure 12(c,d) shows, respectively, the PI and PID experiments at 30 Nm^3/h and temperature plateaus at 220, 400, 730, and 1000 °C. Finally, Figure 12(e,f) shows, respectively, the PI and PID experiments at 50 Nm^3/h and temperature plateaus defined at 180, 500, 750, and 1000 °C.

Qualitatively, it can be seen that the temperature tracking improves with higher air flow rates. This trend, observed in both PI and PID controllers, is associated to the thermal behaviour of the air-heating furnace. High air flow rates enhance heat transfer by convection due to turbulence generation, increasing the heat transfer from the electric resistances to the air. Moreover, air residence time will be lower, decreasing the heat losses through the wall of the heater. It should also be considered that this particular unit has been designed to meet the highest experimental requirements which occur at the highest air flow rates, so its performance is optimized for the highest working air flow range.

Quantitatively, PI and PID controller performances are evaluated depending on the maximum overshoot (MOS) and the settling time (ST). MOS is defined as

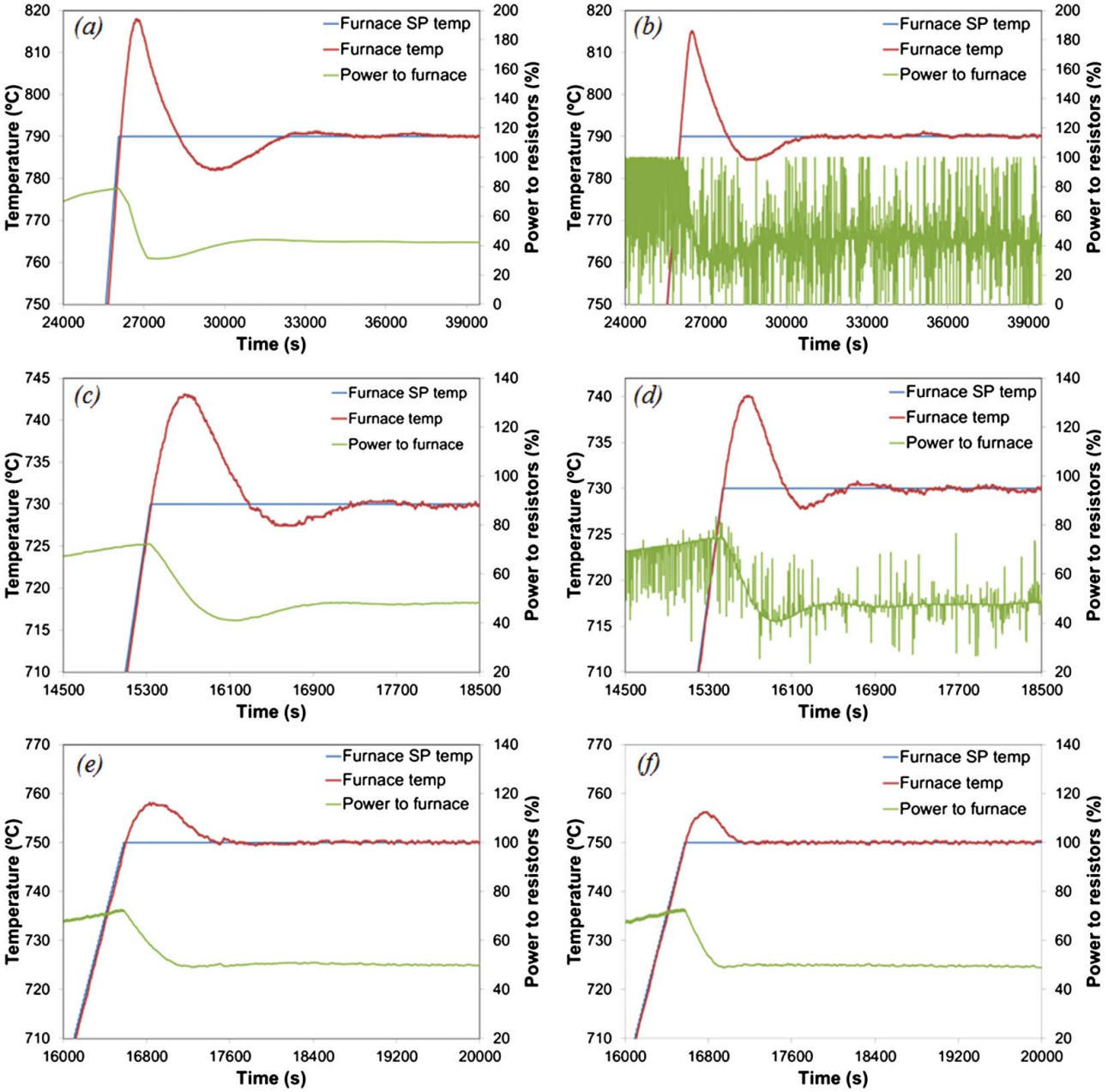

Figure 13. Third temperature plateau using (a) PI and (b) PID controller in the air flow rate interval [10, 20] Nm^3/h. Third temperature plateau using (c) PI and (d) PID controller in the air flow rate interval [20, 40] Nm^3/h. Third temperature plateau using (e) PI and (f) PID controller in the air flow rate interval [40, 60] Nm^3/h.

the difference between the maximum temperature value reached and the temperature setpoint in each temperature plateau. ST is the time required for the temperature to reach and stay into the ±1 °C band around the temperature setpoint.

Table 7. Controllers evaluation for the 10–20 Nm^3/h air flow range.

	PI		PID	
Temperature plateau (°C)	MOS (°C)	ST (s)	MOS (°C)	ST (s)
190	4.97	1062	7.05	460
455	26.59	6314	38.22	6157
790	27.99	7490	25.17	9240
1000	33.63	4076	21.78	2666

Table 8. Controllers evaluation for the 20–40 Nm^3/h air flow range.

	PI		PID	
Temperature plateau (°C)	MOS (°C)	ST (s)	MOS (°C)	ST (s)
220	5.81	1722	7.85	633
400	9.78	1505	9.28	1005
730	13.1	1742	10.09	1024
1000	22.21	3750	14.52	4461

Table 9. Controllers evaluation for the 40–60 Nm^3/h air flow range.

	PI		PID	
Temperature plateau (°C)	MOS (°C)	ST (s)	MOS (°C)	ST (s)
180	3.39	266	2.81	287
500	7.04	718	5.29	350
750	8.18	817	6.28	478
1000	8.75	1379	6.42	803

Results obtained from the analysis of the control experiments are listed in Tables 7–9.

Comparison between air flow ranges shows a general trend in which smaller air flow rates have bigger MOS and ST values. The reason for this behaviour, independently from the control scheme, is that higher air flow rates improve heat transfer processes in the system.

In each particular experiment, there is an upward trend for the MOS and the ST with increasing temperature. This general behaviour, shown for the three air flow ranges in both controllers, is also related to the intrinsic heat transfer process taking place in the test rig, whose complexity is enhanced when more demanding temperatures are required.

Comparing between the two control schemes, PID controllers seem to have better performance than PI controllers do, since they show smaller MOS and ST values. This improvement in the performance should be attributed to the derivative control term and its anticipative action.

Considering that the objective of the installation is the characterization of thermochemical heat storage materials, both control options would be acceptable. Temperature overshoot will seldom be a constraint; as far as temperature setpoint is reached and maintained for a certain period, the materials will react and by doing so, they will be characterized.

In any case, at this point of the analysis, it is also necessary to take into account the controller output behaviour, the variation to the regulator and the power supplied to the furnace resistors. In order to do so, Figure 13 shows the furnace temperature setpoint, the furnace actual temperature and the power supplied to the furnace resistors during the third temperature plateau using the PI and PID controllers at the three air flow rate ranges.

Output behaviour of the PI controllers is similar for the three air flow ranges studied, whereas it depends on the air flow range for the PID controllers. For the highest range, PI and PID output performances are comparable, but with lower air flow ranges, PID controllers' outputs show bigger and more frequent variations between consecutive signals.

This behaviour is known as derivative kick and it is an undesirable behaviour for PID controllers. As it is shown in Figure 13(d,f), the importance of the derivative kick increases with lower air flow rates; the intrinsic heat transfer processes become more complex and slower, therefore, the system is more difficult to control.

Here, the derivative kick behaviour does not affect overall PID control performance since the gathered MOS and ST are smaller than the ones found for the PI control. However, in any cases, it will eventually have a negative impact on the resistors, whose useful life is reduced.

Therefore, aiming to maximize the installation lifetime, while observing the temperature accuracy required, PID controllers would be considered for the highest air flow rates, and PI controllers would be applied for the intermediate and lower air flow rate ranges. In the exceptional cases in which the evaluated material may have special accuracy requirements, PID controllers would be considered for the intermediate air flow rate range, and in very rare cases for the lowest air flow rate interval.

5. Conclusions

The air heating furnace control developed grants great flexibility to the 100-Wh multi-purpose particle reactor, for thermochemical heat storage evaluation in concentrating solar power plants. By providing air mass flow rates between 10 and 60 Nm^3/h at temperatures from ambient up to 1000 °C, the test rig will allow for the evaluation of different parameters for thermochemical storage such as reaction yield, particle size, and successive oxidation/reduction cycles on the process cyclability, the mechanical strength and abrasion resistance of the storage materials.

The D&C techniques applied have simplified the control design of a MISO nonlinear plant to a SISO linear plant. By discretizing working air flow rates as well as temperatures in intervals, a multiple controller has been designed, optimized and tested under real conditions.

Aiming to achieve the temperature accuracy required while maximizing the installation lifetime, PID controllers will be of application for the highest air flow rate, and PI controllers would be applied for the intermediate and lower air ranges. In exceptional cases in which the evaluated material may have higher accuracy requirements, PID controllers would be considered for the intermediate air flow range, and in very rare cases, for the lowest air flow range.

From the control performance evaluation done, the set of 12 PI and PID controllers have been defined to meet the application requirements. It has been demonstrated that the air temperature control developed meets the performance required for the material characterization experiments.

Acknowledgments

Authors would like to thank the European Commission which supported this facility construction in the framework of the European project TCS Power, "Thermochemical Energy Storage for Concentrated Solar Power Plants". FP7-Cooperation. Call identifier: FP7-ENERGY-2011-1. J. González-Aguilar also wishes to thank the Spanish Ministry of Science and Innovation (grant Plan Nacional ENE2011-29293). J.G. Mollocana Lara also wishes to thank the Ecuadorian SENESCYT (Secretaría nacional de educación superior, ciencia y tecnología) for the grant n° 081-2012, and S Álvarez de Miguel also wishes to thank the Escuela Técnica Superior de Ingeniería y Diseño Industrial for the grant n° 201600018266.

Disclosure statement

No potential conflict of interest was reported by the authors.

Funding

European Commission [grant number FP7-ENERGY-2011-1]; Ministerio de Ciencia Tecnología y Telecomunicaciones [grant number ENE2011-29293]; Secretaría Nacional de Educación Superior, Ciencia y Tecnología [grant number 081-2012]; Escuela Técnica Superior de Ingeniería y Diseño Industrial [grant number 201600018266].

ORCID

S. Álvarez de Miguel http://orcid.org/0000-0002-7038-886X

References

[1] Shamsuzzoha M, Skogestad S. The setpoint overshoot method: a simple and fast closed-loop approach for PID tuning. J Process Control. 2010;20(10):1220–1234.
[2] Vanavil B, Chaitanya KK, Rao AS. Improved PID controller design for unstable time delay processes based on direct synthesis method and maximum sensitivity. Int J Syst Sci. 2013;46:1349–1366.
[3] Sarhan H. A software-based gain scheduling of PID controller. Int J Instrum Control Syst. 2014;4(3):1–10.
[4] Sakthivel G, Anandhi TS, Natarajan SP. Modelling and real time implementation of digital PI controller for a nonlinear process. J Innov Res Eng Sci. 2011;2(5):274–290.
[5] Yu Y, Zhang Y, Yuan X, et al. A LabVIEW-based real-time measurement system for polarization detection and calibration. Optik (Stuttg). 2014;125:2256–2260.
[6] Han Y, Jinling J, Guangjian C, et al. Temperature control of electric furnace based on fuzzy PID. International Conference on Electronics and Optoelectronics; 2011; Dalian, China.
[7] Lu D, Wang JX, Li JF. The temperature control of electric furnace based on PID genetic algorithm. Adv Mater Res. 2012;490–495:828–834.
[8] Dingdu W. Electric furnace control system based on the grey prediction fuzzy adaptive control. Sixth International Conference on Fuzzy Systems and Knowledge Discovery. Vol. 4; USA: IEEE Conference Publications; 2009. p. 86–90.
[9] Mohamad S, Ishak AA, Aishah S, et al. Design of fuzzy logic controller for overdamped temperature response of a process air heater system. Fourth International Conference Modeling, Simulation and Applied Optimization. USA: IEEE Conference Publications; 2011. p. 1–4.
[10] Thyagarajan T, Shanmugam J, Ponnavaikko M, et al. Advanced control schemes for temperature regulation of air heat plant. IEEE International Fuzzy Systems Conference Proceedings, No. II. USA: IEEE Conference Publications; 1999. p. 767–772.
[11] Kano M, Ogawa M. The state of the art in chemical process control in Japan: good practice and questionnaire survey. J Process Control. 2010;20(9):969–982.
[12] Sung SW, Lee J, Lee I-B. Process identification and PID control. 1st Ed. IEEE Press; 2009. ISBN: 978-0-470-82410-8.
[13] Kusters A, Ditzhuijzen GAJM. MIMO system identification of a slab reheating furnace. Proceedings of the Third IEEE Conference on Control Applications. Vol. 3. USA: IEEE Conference Publications; 1994. p. 1557–1563.
[14] O'Dwyer A. Handbook of PI and PID controller tuning rules. 3rd ed. London: Imperial College Press; 2009.
[15] Wörner A, Binyami S, Giger F, et al. The TCS power project thermochemical energy storage for concentrated solar power plants. In Proceedings of Solar Paces; 2012; Marrakech, Morocco.
[16] Álvarez De Miguel S, Gonzalez-Aguilar J, Romero M. 100-Wh multi-purpose particle reactor for thermochemical heat storage in concentrating solar power plants. Energy Proc. 2013;49:676–683.
[17] Álvarez De Miguel S, Bellan S, García De María JM, et al. Numerical modelling of a 100-Wh lab-scale thermochemical heat storage system for concentrating solar power plants. AIP Conference Proceedings. Vol. 1734. 2016. p. 50005.
[18] Mollocana Lara JG. Desarrollo del control de proceso en un banco de ensayos de reactores de partículas a alta temperatura [Control process development for a high temperature particle reactor]. Madrid, Spain: Universidad Politécnica de Madrid; 2013.